A detailed View on the Trapezoidal Operation for MMC Type Braking Chopper in Medium Voltage Application

Patrick Hofstetter, Viktor Hofmann, Dennis Karwatzki
Siemens AG, Large Drives Applications
Vogelweiherstraße 1-15
90441 Nürnberg, Germany
+49 152 38939179
Email: Patrick.Hofstetter@siemens.com
URL: http://www.siemens.com

Keywords

≪Modular Multilevel Converters (MMC)≫, ≪Control of drive≫, ≪Industrial application≫, ≪Reliability≫, ≪Braking Chopper≫

Abstract

A detailed view on the trapezoidal operation of the modular multilevel converter (MMC) type braking chopper is given. The influence of different limitations on the possible operational range is derived and an optimization algorithm is suggested. Finally, the analysis is verified on an exemplary medium voltage application and validated by simulation.

Introduction

Braking choppers are typically applied in drive systems having only two-quadrant (2Q) operation to provide motor braking capability. Furthermore, they can be used in converter systems for protection against high voltages, which may occur when a load feeds back energy into the converter. The easiest way to realize a braking chopper is using a switch in series with a braking resistor, see Fig. 1 (I).

By applying this circuit to the DC-link, electrical energy can simply be converted into heat in the braking resistor R_{BR} by closing the switch. A Modular Multilevel Converter (MMC) is shown on the left side of Fig. 1 and is often equipped with half bridge submodules (a). As the MMC is typically used in high and medium voltage applications, the standard braking chopper is usually not applied, as this would result in large quantities of high blocking semiconductors connected in series to realize the switch. The typical static and dynamic voltage imbalances between these semiconductors would have to be minimized by selecting IGBTs with low parameter deviations such as e.g. leakage current or threshold voltage. Additionally, passive snubbers or active methods are probably needed. In medium voltage applications a high blocking SiC MOSFET [1] may be applicable in future to replace the series connection. Another problem of a conventional braking chopper at an MMC is the influence of the arm inductances L_{arm}, which induce overvoltages at turn-off events during the braking chopper operation. Therefore, in literature braking chopper topologies based on modular cells were presented and analysed for MMC applications. One way is to use the submodules with distributed braking resistors $R_{\mathrm{BR,dis}}$ such as (b) directly in the MMC instead of the common half bridge submodules (a). The submodules with resistors can alternatively be equipped into an external braking chopper arm (II) with or without an external braking resistor R_{BR}. The advantage of submodules with integrated braking resistor is the possibility to easily discharge the submodule capacitor and thus to simply achieve energy balance in the cells. The disadvantages of the resistor submodules are typically higher costs due to higher hardware efforts and the necessity to cool the distributed resistors. These kind of braking chopper topologies are for example being analyzed

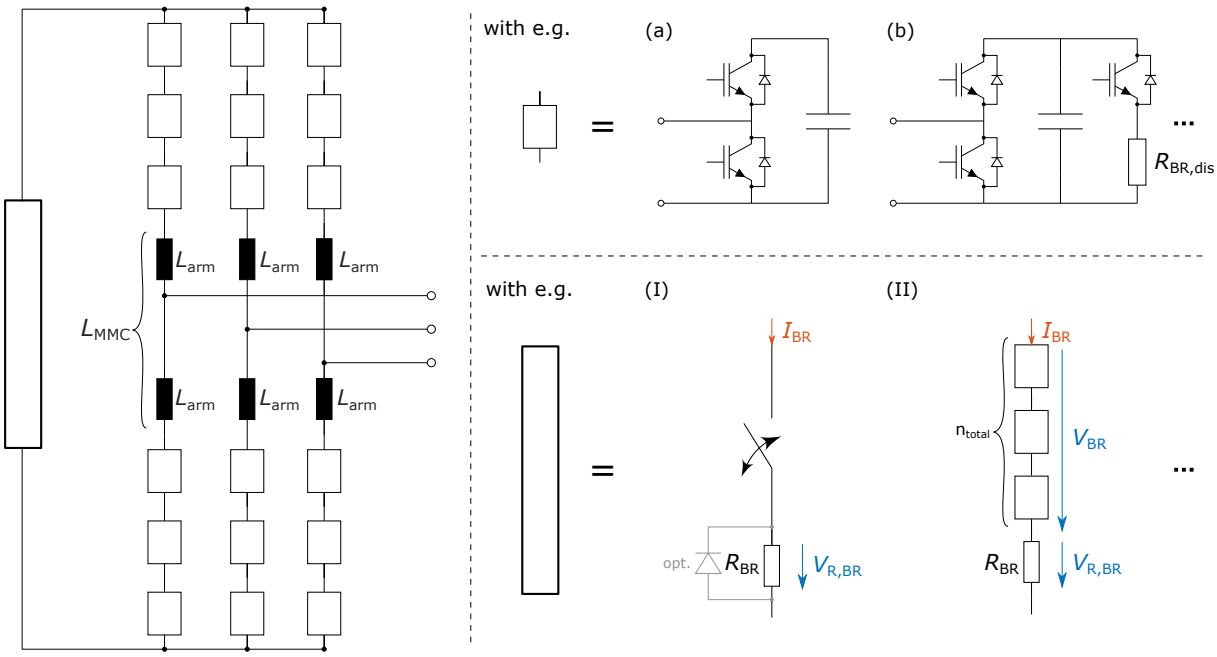

Fig. 1: MMC Converter and different types of half bridge submodules as well as braking chopper topologies such as (a) half bridge submodule, (b) half bridge submodule with distributed chopper resistor $R_{BR,dis}$, (I) Classical braking chopper or (II) MMC type braking chopper

in [2, 3, 4, 5, 6, 7]. The main advantage of using common half bridge submodules (a) in both MMC and external braking chopper arm (II) is the reduction in component variety. Consequently, complexity in production lines and costumer service efforts are minimized. Accordingly, only the submodule type (a) for both the MMC and the MMC type braking chopper (II) is analyzed in this paper. An equivalent circuit diagram with the voltage definitions is given in Fig. 2.

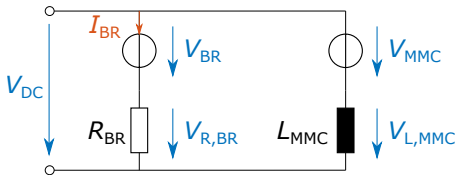

Fig. 2: Equivalent circuit diagram corresponding to the MMC of Fig. 1 with MMC type braking chopper (II), which is equipped with bridge modules (a)

In the braking chopper path, the voltages consist of the modulated voltage of the braking chopper cells V_{BR} and the voltage drop across the braking resistor $V_{R,BR}$. The MMC is represented by the modulated DC voltage V_{MMC} and the voltage drop across the effective DC side arm inductance $V_{L,MMC}$. There are two possible ways to operate the chopper to achieve energy balance in the cells. On the one hand, you can use a continuous operation, where the energy balancing is done by circulating currents, as shown in [7, 8]. On the other hand, there is the possibility to drive a trapezoidal braking current, which is shown in [2, 6, 9]. The focus of this paper is on the latter operation. In contrast to previous publications a detailed view on the limitations and the maximum possible operation ranges is shown.

In order to simplify following explanations, the possible switching states of the half bridge submodules is defined in Table. I.

Table I: Submodule switching states of the half bridge submodules from Fig. 1(a)

switching state	upper IGBT	lower IGBT	voltage
S_0	off	on	0
S_1	on	off	$V_{\mathrm{C,SM}}$
S_2	off	off	0 @ neg. I $V_{\mathrm{C,SM}}$ @ pos. I

Operation principle

When the current demand for the braking choppper $I^*_{\mathrm{BR,RMS}}$ is greater than zero, an active braking chopper operation is performed. The main part of the power is dissipated in the resistor during t_{on}, when all n_{total} submodules of the chopper are in S_0 ($V_{\mathrm{BR}} = 0\,\mathrm{V}$). This is schematically illustrated in the operation principle in Fig. 3.

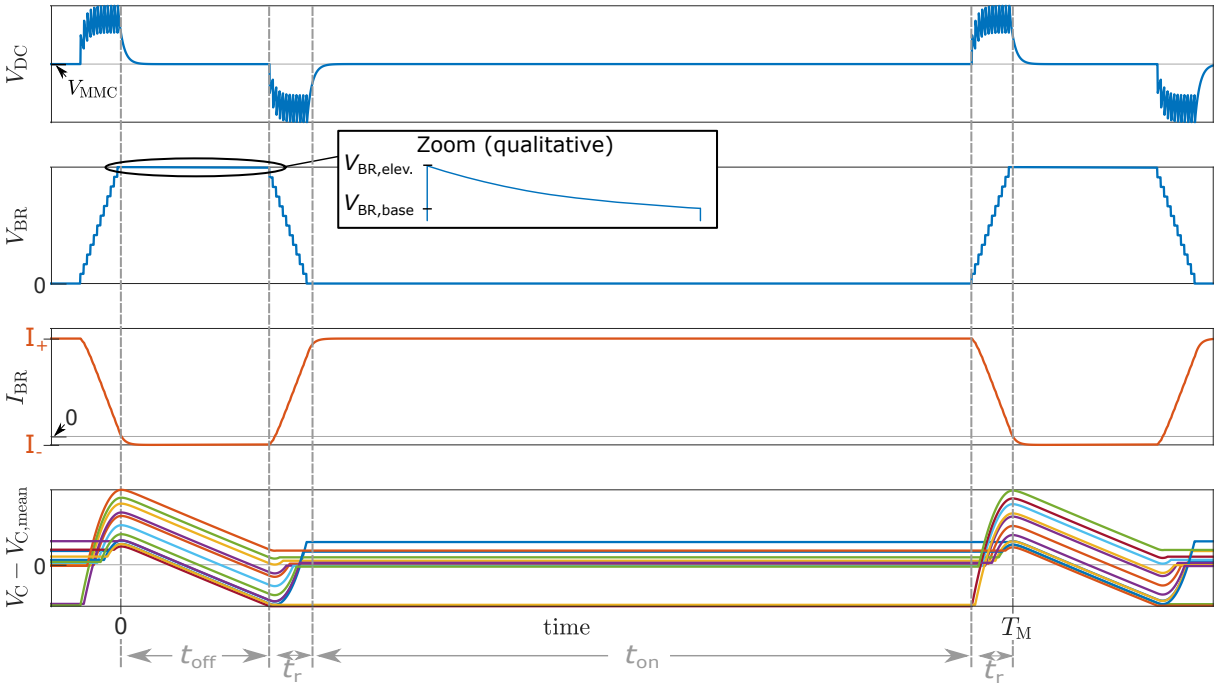

Fig. 3: Trapezoidal operation principle of the braking chopper during active operation based on simulation for $n_{\mathrm{total}} = 12$

During the voltage ramps (with t_{r}), the capacitor voltages of the cells will be charged, when $V_{\mathrm{BR}} < V_{\mathrm{DC}}$. When all the modules are in S_1, the braking chopper cells are discharged, as long as $V_{\mathrm{BR}} > V_{\mathrm{DC}}$. In order to keep the cell voltages below their maximum voltage rating and to ensure an energy balance, there is a minimum time $t_{\mathrm{off,min}}$ for this chopper state. As the capacitor voltages of the braking chopper submodules must stay balanced, the switching order should be done as explained in [9]. When the cells switch from S_1 to S_0, the order is from highest to lowest V_{C}. In contrast to this, when the cells switch from S_0 to S_1, the order is from lowest to highest.

When the braking chopper is not needed for energy dissipation it should be in an idle mode, which is explained below. When the current demand for the braking chopper is zero ($I^*_{\mathrm{RMS}} = 0\,\mathrm{A}$), the braking chopper enters the idle mode, where it should waste as few energy as possible. There is the possibility to simply keep all the cells in S_1. Essentially, the braking chopper path would correspond to a series connection of the submodule capacitors and the braking resistor. Considering an operation of an MMC with a diode rectifier, the rectifier's voltage ripple would cause relevant currents and losses in the braking

resistor. Another solution to achieve low losses in idle mode is to set all the submodules into S_2. This way the submodule capacitors can only be charged by V_{DC} but not discharged by it, but there would still be the problem of voltage balancing between the cells. MMC submodules are typically equipped with balancing and discharge resistors in parallel to the IGBTs and capacitor, respectively. These resistors already help to achieve a better balance in capacitor voltages. Additionally, it is proposed to keep the submodule with the highest capacitor voltage in S_0. This can for example be checked every modulation cycle T_M, so that the appropriate submodule can slowly be discharged by the discharge and balancing resistors, whereas the other modules are charged to V_{DC}. The proposed switching states during active operation and idle mode are summarized in Fig. 4.

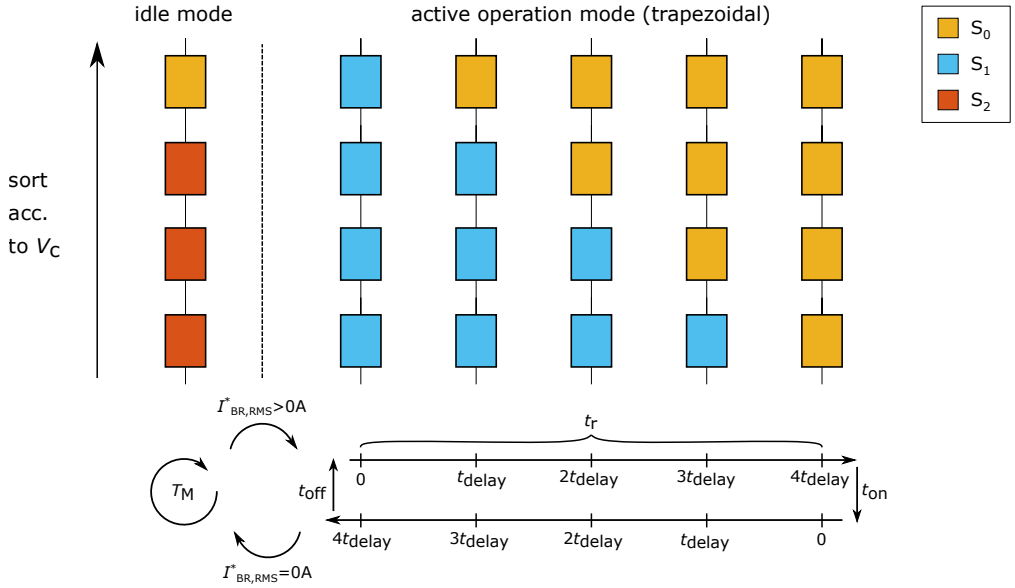

Fig. 4: Switching states during active and idle mode for $n_{total} = 4$ submodules in the braking chopper

Design Optimization

Without the need of cell energy balance, the maximum dissipated power $P_{R,BR,max}$ at a specific V_{DC} would only be limited by the maximum admissible RMS current I_{nom} of the submodules, by choosing $R_{BR} = V_{DC}/I_{nom}$. In the following, the determination of $P_{R,BR,max}$ and the corresponding R_{BR} at a specific V_{DC} will be derived under consideration of energy balancing and thus the presence of a minimum chopper off-state $t_{off,min}$ to discharge the braking chopper cells. The influence of these additional limitations will then be derived. Finally, the possible operating range for an exemplary medium voltage application will be shown and the results will be validated by simulation.

Determination of the maximum dissipation power

The power which is dissipated in one modulation period T_M can simply be controlled by the duty cycle and is calculated by

$$P_{R,BR} = I_{BR,RMS}^2 \cdot R_{BR}. \tag{1}$$

To determine $P_{R,BR,max}$, the maximum RMS current of the trapezoidal current profile (compare Fig. 3) is estimated by

$$I_{BR,RMS,max} = \sqrt{f_M \cdot \left[\frac{2t_r \left(I_+^3 - I_-^3\right)}{3\left(I_+ - I_-\right)} + I_+^2 \cdot \underbrace{\left(T_M - t_{off,min} - 2t_r\right)}_{t_{on,max}} + I_-^2 \cdot t_{off,min} \right]}, \tag{2}$$

where I_+ and I_- describe the maximum positive and negative braking chopper currents, respectively and f_M the modulation frequency. In order to determine $t_{off,min}$, the discharged energy during this time has to be equal to the charged energy during the ramps. During t_{on} the braking chopper submodule capacitors are only insignificantly discharged by the discharge and balancing resistors. Therefore, it has no effect on the determination of $t_{off,min}$. The voltage levels of the braking chopper before and after the charging of the ramps are called $V_{BR,base}$ and $V_{BR,elev.}$, respectively and can be seen in the "zoom" of Fig. 3. The initial sum of submodule capacitor voltages at step zero ($i = 0$) is given by

$$V_{C,total,0} = V_{BR,base} = n_{total} \cdot V_{C,nom} \tag{3}$$

with the nominal voltage of the braking chopper submodules $V_{C,nom}$. The voltage after the ramps $V_{BR,elev.}$ can be calculated by evaluating the sum of the submodule capacitor voltages $V_{C,total,i+1}$ for each single step i of the consecutive switching of the cells from $n = n_{total} - 1$ active submodules to $n = 1$ and back to $n = n_{total} - 1$. Depending on the sum of voltages of the activated submodules, the capacitors are charged or discharged. If the voltage of the active submodules is higher than V_{DC}, they discharge and the voltage after one step with t_{delay} is calculated by

$$V_{C,total,i+1} = V_{DC} + (V_{C,total,i} - V_{DC}) \cdot e^{-\frac{t_{delay}}{R_{BR} \cdot C/n}} \tag{4}$$

with the submodule capacitance of C. Most of the time, the sum of voltages of the active cells is lower than V_{DC} during the ramps. Hence, the submodule capacitors are charged. In this case the calculation of the voltage after one step can be performed by

$$V_{C,total,i+1} = V_{DC} \cdot \left(1 - e^{-\frac{t_0 + t_{delay}}{R_{BR} \cdot C/n}}\right) \tag{5}$$

with

$$t_0 = -\ln\left(1 - \frac{V_{C,total,i}}{V_{DC}}\right) \cdot R_{BR} \cdot C/n. \tag{6}$$

The last step's $V_{C,total,i+1}$ corresponds to $V_{BR,elev.}$, which should discharge exactly to the base level $V_{BR,base}$ during $t_{off,min}$, compare „zoom" in Fig. 3. The value of $t_{off,min}$ can therefore be calculated by

$$t_{off,min} = -\ln\left(\frac{V_{BR,base} - V_{DC}}{V_{BR,elev.} - V_{DC}}\right) \cdot R_{BR} \cdot C/n_{total}. \tag{7}$$

Choice of submodule capacitance

Along with the value of the braking resistor, the submodule capacitance C may be a variable, which can typically be chosen freely, but influences $P_{R,BR,max}$. On the one hand lower capacitance values seem to lead to a smaller $t_{off,min}$ according to (7), as the cell capacitor discharge is faster due to a smaller time constant. On the other hand $V_{BR,elev}$ of the equation will also be higher for lower capacitances. Mainly, this is influenced by the steps calculated in (5) with (6). In principal, a lower C and thus a smaller time constant leads to a faster charge but also a faster discharge of the capacitors, which finally cancels each other out when considering $P_{R,BR,max}$. Consequently, less submodule capacitors can be used compared to the MMC submodules, which saves costs. But one has to keep in mind that a lower capacitance results in a higher submodule voltage during the charging process, which must not exceed the over voltage limit of the submodule.

Influence of limitations on the operating area

For a given system, the possible operating area of the braking chopper can be described by $I_{\mathrm{BR,RMS,max}}$ and the specific resistance

$$R_{\mathrm{spec}} = \frac{R_{\mathrm{BR}}}{V_{\mathrm{DC}}}. \tag{8}$$

Without further limitations, the maximum current is given by $V_{\mathrm{DC}}/R_{\mathrm{BR}}$, compare blue curve in Fig. 5.

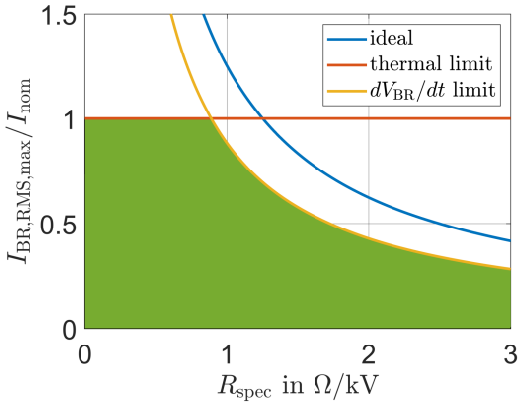

Fig. 5: Possible operating area for the trapezoidal braking chopper operation

This would be the case, if all submodules would be switched at the same time ($t_{\mathrm{delay}} = 0$ & $t_{\mathrm{r}} = 0$) and if there wouldn't be the need of a minimum off time of the braking chopper. As explained in the introduction, switching the submodules at once leads to high overvoltages at the DC link due to the arm inductances. This is simply described by

$$V_{\mathrm{DC}}(t) = V_{\mathrm{MMC}} + V_{\mathrm{C,total}} \cdot e^{-\frac{R_{\mathrm{BR}}}{L_{\mathrm{MMC}}} \cdot t}. \tag{9}$$

Due to the consecutive switching, this changes to

$$V_{\mathrm{DC}}(t) = V_{\mathrm{MMC}} + \sum_{n=0}^{n_{\mathrm{total}}-1} \boldsymbol{H}(t - n \cdot t_{\mathrm{delay}}) \cdot V_{\mathrm{C,n}} \cdot e^{-\frac{R_{\mathrm{BR}}}{L_{\mathrm{MMC}}} \cdot (t - n \cdot t_{\mathrm{delay}})} \tag{10}$$

with the Heaviside function $\boldsymbol{H}(t)$. An example was already shown in the first plot of Fig. 3. The consecutive switching is basically used to reduce $\frac{dV_{\mathrm{BR}}}{dt}$ and thus the $\frac{dI_{\mathrm{BR}}}{dt}$ consequently lowering overvoltages on V_{DC}. The current limitation due to $t_{\mathrm{off,min}}$ can therefore be interpreted as a $\frac{dV_{\mathrm{BR}}}{dt}$ limitation. According to the calculation with the equations (2)-(7), this reduces the theoretical maximum RMS current to the values given by the yellow curve in Fig. 5. This gets worse for higher modulation frequencies. But the lower f_{M}, the higher is the voltage ripple of the MMC cell capacitors. Therefore, a minimum modulation frequency is needed to ensure a stable drive operation.

The thermal limits are additional factors limiting the maximum possible RMS current, compare the red curve in Fig. 5. To keep it simple in this paper, it considers a thermal limit which is given by the mechanical components of the submodule. The resulting possible operating area is illustrated in green. In order to maximize the possible power of the braking chopper, the resistor value and current should be as high as possible, compare (1). This is given by the intercept point of the two limiting curves. This point can easily be determined by iteration:

As a reasonable starting value for R_{BR}, $V_{\mathrm{DC}}/I_{\mathrm{max}}$ is used with the maximum absolute peak current rating of the submodules I_{max}. $I_{\mathrm{BR,RMS,max}}$ is determined according to the calculation with the equations (2)-(7). R_{BR} is then increased until

$$I_{\mathrm{BR,RMS,max}} = I_{\mathrm{nom}} \tag{11}$$

with the nominal current of the submodules I_{nom}. This way, the algorithm follows the yellow curve of Fig. 5 from a reasonable starting point to the intercept with the thermal limit. Finally, $P_{\text{R,BR,max}}$ is calculated by (1).

Example of a medium voltage application and validation by simulation

The MMC type braking chopper should be used in medium voltage application. A number of MMCs operating at different modulated DC voltages V_{MMC} should be equipped with braking choppers. The specifications of one half bridge submodule are given in Table II.

Table II: Specifications of a half bridge submodule based on a medium voltage application

	value	description
$V_{\text{C,nom}}$	1kV	nominal cell voltage
I_{nom}	1kA	nominal RMS current
I_{max}	2kA	absolute maximum peak current rating
t_{delay}	10µs	time between consecutive switching steps
C_{mod}	2mF	capacitor value of the submodule

The chopper modulation frequency is set to $f_{\text{M}} = 600\,\text{Hz}$ to meet the MMC cell voltage ripple requirements. The arm inductance of the MMC is presumed to be $L_{\text{MMC}} = 100\,\mu\text{H}$. The braking chopper voltage rise/drop of about

$$\frac{dV_{\text{BR}}}{dt} = \frac{V_{\text{C,nom}}}{t_{\text{delay}}} = 0.1\,\text{kV}/\mu\text{s} \tag{12}$$

is assumed to be low enough to not develop critical $\frac{dI_{\text{BR}}}{dt}$ and thus voltages in this inductance. For various V_{MMC}, the results with different numbers of submodules (SM) are shown in Fig. 6a).

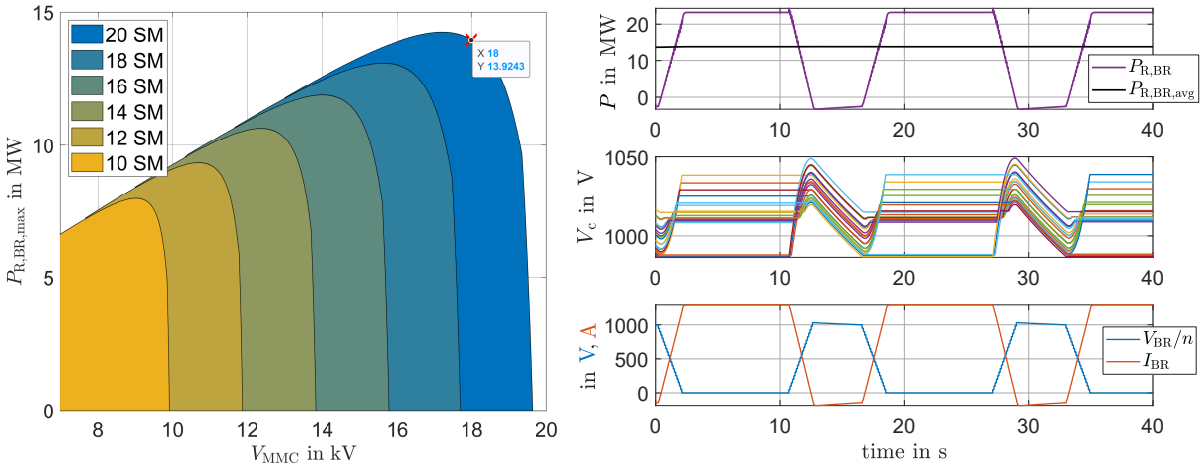

(a) Possible operating range for the MMC braking chopper (b) Simulation result for $n = 20$ at $V_{\text{MMC}} = 18\,\text{kV}$ at the maximum duty cycle

Fig. 6: Calculation and simulation results for the considered application

The individual plots can be optically divided into two parts. On the left side of the maximum in Fig. 6(a), the maximum power is essentially limited by I_{nom} of the submodules. The right side shows the effect of higher $t_{\text{off,min}}$. To validate the calculation, different operation points were simulated successfully. For example, Fig. 6(b) shows the operation point with $n = 20$ submodules at $V_{\text{MMC}} = 18\,\text{kV}$ with an optimized $R_{\text{BR}} = 13.94\,\Omega$. On the one hand, it can be seen that the average power of 13.81 MW matches very well with the calculation of 13.92 MW. On the other hand, the cell voltages and thus the energy of the braking

chopper cells does not increase over time and matches with $V_{\mathrm{C,nom}}$ of about 1 kV. When a lower duty cycle is needed, the cell voltage level would be lower as the discharge phase during t_{off} would be longer.

Conclusion

The trapezoidal operation of the MMC type braking chopper was analyzed in detail. First, the operation principle was explained and the determination of the maximum braking chopper power was analyzed. With this, the influence of the consecutive switching and thermal limits were shown and an optimization algorithm was derived. Based on these calculations, the possible operating range was derived for an exemplary medium voltage application and finally validated by simulation results.

References

[1] K. Vechalapu, S. Bhattacharya, E. Van Brunt, S. Ryu, D. Grider, and J. Palmour, "Comparative evaluation of 15-kv sic mosfet and 15-kv sic igbt for medium-voltage converter under the same dv/dt conditions," *IEEE Journal of Emerging and Selected Topics in Power Electronics*, vol. 5, no. 1, pp. 469–489, 2017.

[2] B. Xu, C. Gao, J. Zhang, J. Yang, B. Xia, and Z. He, "A novel dc chopper topology for vsc-based offshore wind farm connection," *IEEE Transactions on Power Electronics*, vol. 36, no. 3, pp. 3017–3027, 2021.

[3] V. Hussennether, J. Rittiger, A. Barth, D. Worthington, G. Dell'Anna, M. Rapetti, B. Hühnerbein, and M. Siebert, "Projects borwin2 and helwin1 – large scale multilevel voltage-sourced converter technology for bundling of offshore windpower," in *CIGRÉ Session - B4-306*, pp. 1–11, 2012.

[4] Y. Okazaki, S. Shioda, and H. Akagi, "Performance of a distributed dynamic brake for an induction motor fed by a modular multilevel dscc inverter," *IEEE Transactions on Power Electronics*, vol. 33, no. 6, pp. 4796–4806, 2018.

[5] M. Wang, Y. Hu, W. Zhao, Y. Wang, and G. Chen, "Application of modular multilevel converter in medium voltage high power permanent magnet synchronous generator wind energy conversion systems," *IET Renewable Power Generation*, vol. 10, no. 6, pp. 824–833, 2016.

[6] J. Maneiro, S. Tennakoon, C. Barker, and F. Hassan, "Energy diverting converter topologies for hvdc transmission systems," in *2013 15th European Conference on Power Electronics and Applications (EPE)*, pp. 1–10, 2013.

[7] A. Birkel, A. Schön, and M. Bakran, "Analysis and semiconductor based comparison of energy diverting converter topologies for hvdc transmission systems," in *2015 17th European Conference on Power Electronics and Applications (EPE'15 ECCE-Europe)*, pp. 1–10, 2015.

[8] V. Hofmann and P. Hofstetter, "Design and modulation optimization of an mmc based braking chopper," in *2022 24th European Conference on Power Electronics and Applications (EPE'22 ECCE Europe)*, pp. 1–7, 2022.

[9] S. Schoening, P. K. Steimer, and J. W. Kolar, "Braking chopper solutions for modular multilevel converters," in *Proceedings of the 2011 14th European Conference on Power Electronics and Applications*, pp. 1–10, 2011.